

Fast and Robust Subspace Clustering Using Random Projections

Guangcan Liu, *Member, IEEE*, Qingshan Liu, *Senior Member, IEEE*,
Yubao Sun, Zhao Zhang, *Senior Member, IEEE*, and Meng Wang



Abstract—Over the past several decades, subspace clustering has been receiving increasing interest and continuous progress. However, due to the lack of scalability and/or robustness, existing methods still have difficulty in dealing with the data that possesses simultaneously three characteristics: high-dimensional, massive and grossly corrupted. To tackle the scalability and robustness issues simultaneously, in this paper we suggest to consider a problem called *compressive robust subspace clustering*, which is to perform robust subspace clustering with the compressed data, and which is generated by projecting the original high-dimensional data onto a lower-dimensional subspace chosen at random. Given these random projections, the proposed method, *row space pursuit* (RSP), recovers not only the authentic row space, which provably leads to correct clustering results under certain conditions, but also the gross errors possibly existing in data. The compressive nature of the random projections gives our RSP high computational and storage efficiency, and the recovery property enables the ability for RSP to deal with the grossly corrupted data. Extensive experiments on high-dimensional and/or large-scale datasets show that RSP can maintain comparable accuracies to prevalent methods with significant reductions in the computational time.

Index Terms—clustering, subspace, compressive sensing, scalability, robustness

1 INTRODUCTION

Benefiting from the increases in data and computational power, supervised learning has accomplished considerable strides in recent years. However, it is almost impossible to solve *unconstrained* recognition problems (e.g., wild face recognition) by endlessly increasing labeled samples, as the sample space of an unconstrained problem is essentially an infinite

set. To break through the limit of supervised learning, unsupervised (resp. weakly-supervised) learning, which aims at learning the extrinsic structures underlying data with no (resp. little) label information, is a promising direction. Among various unsupervised problems, *subspace clustering* [1], the task of grouping together the data points lying approximately on the same (linear) subspace, is a representative one. In certain cases, actually, unsupervised learning can be formulated as a subspace clustering problem [2].

Due to its significance in science and prospects in application, subspace clustering has received extensive attentions in the literatures, e.g., [3–26] (see a brief survey in next section). However, existing methods still have difficulty to deal with the data arising from today’s data-driven community, which raises challenges in at least two modalities:

- *Scalability*: In computer vision and image processing, the data dimension (denoted as m) and the number of data points (denoted as n) could be both huge, e.g., in millions or larger. Given this pressing situation, it is crucial to develop efficient subspace clustering methods that scale only linearly in both m and n .
- *Robustness*: Due to the unconstrained nature of today’s data acquisition procedure, the observed data is often full of gross errors, e.g., corruptions, outliers and missing measurements. It is also an urgent need to establish robust methods that are able to automatically correct the gross errors possibly existing in data.

Lots of methods have been proposed to address the above two challenges, e.g., [13, 14, 16, 19–21, 25, 27]. In general, these methods contribute to only one aspect of either robustness or scalability, not both of them. For example, Low-Rank Representation (LRR) [13, 22] and its extensions can handle gross errors to some extent, but involve computationally expensive steps, such as the construction of $n \times n$ affinity matrices and the spectral partition of n -node graphs. The methods established in [20, 21, 25, 28] scale linearly in n or even both m and n , but possess no ability to recover the clean data from grossly corrupted observations.

- G. Liu is with B-DAT and CICAET, School of Information and Control, Nanjing University of Information Science and Technology, Nanjing, China 210044. Email: gcliu@nuist.edu.cn.
- Q. Liu is with B-DAT, School of Information and Control, Nanjing University of Information Science and Technology, Nanjing, China 210044. Email: qslu@nuist.edu.cn.
- Y. Sun is with B-DAT and CICAET, School of Information and Control, Nanjing University of Information Science and Technology, Nanjing, China 210044. Email: sunyb@nuist.edu.cn.
- Z. Zhang is with School of Computer Science and Technology, Soochow University, Suzhou, China 215006. Email: cszhang@gmail.com.
- M. Wang is with School of Computer Science and Information Engineering, Hefei University of Technology, 193 Tunxi Road, Hefei, Anhui, China 230009. E-mail: eric.mengwang@gmail.com.

In fact, there is a certain inevitability that existing methods cannot address the scalability and robustness issues at the same time:

- The high computational cost is directly attributable to the high-dimensional and massive nature of data. Thus, to improve the computational efficiency of subspace clustering methods, it is straightforward to decrease m and/or n .
- To identify the gross errors in data, however, it is in fact very beneficial that both m and n are huge [23]. Thus, in a sense of robustness, we may need to preserve m and n .

To resolve such a contradiction, we would suggest to consider a problem called *compressive robust subspace clustering*, which is defined as follows:

Problem 1.1 (Compressive Robust Subspace Clustering). Let $X = [x_1, \dots, x_n] \in \mathbb{R}^{m \times n}$ store a collection of n m -dimensional points approximately drawn from a union of k subspaces. Suppose that $R \in \mathbb{R}^{p \times m}$ ($p \ll m$) is a sensing matrix generated at random, e.g., random Gaussian. Denote $M \triangleq RX \in \mathbb{R}^{p \times n}$. Given M and R , segment all points into their respective subspaces and identify the gross errors possibly existing in X as well.

The above problem, in general, combines the spirits of *robust subspace clustering* [12, 13, 18] and *compressive sensing* [29]. Intuitively, a solution to Problem 1.1 may relieve the issues of scalability and robustness simultaneously: The dimension reduction operator reduces the number of variables under consideration and can therefore diminish the cost of computation. On the other hand, the purpose of error correction coincides with the essence of robustness. Unfortunately, in the presence of gross errors, Problem 1.1 is indeed challenging and cannot be solved by simply inputting M into existing methods such as LRR. This is because dimension reduction could change the statistical properties of the errors. For example, consider the case where the gross errors are entry-wisely sparse, i.e., only a small fraction of the entries in X are grossly corrupted. In the compressed matrix M , however, the errors may spread to every entries of the matrix, i.e., the errors in M become dense. What is more, most existing data recovery methods, e.g., Principal Component Pursuit (PCP) [30] and LRR, rely on the *blessing of dimensionality* [23], which could be violated by dimension reduction. Due to these key features, Problem 1.1 is essentially different from the *compressive subspace clustering* problem studied in [31, 32].

To study Problem 1.1, we further propose a novel method termed *row space pursuit* (RSP). Given the compressed matrix M and sensing matrix R , RSP recovers not only the row space of the clean data but also the possible gross errors. Since the authentic row space (i.e., row space of clean data) provably determines the true subspace membership of the data points, the final clustering results are obtained by simply using the recovered row space as input to

perform K-Means clustering. In general, RSP owns a computational complexity of only $O(mnp)$ and can therefore fast segment a large number of high-dimensional data points. Furthermore, most of the computational resources required by RSP are spent on matrix multiplications, which are easy to accelerate by parallel algorithms. Extensive experiments demonstrated on four high-dimensional and/or large-scale datasets show that RSP is much more efficient than the prevalent methods while achieving comparable or even more accurate clustering results.

2 RELATED WORK

Lots of subspace clustering methods have been proposed and investigated in the literature. Early methods, e.g., Random Sample Consensus (RANSAC) [3], K-Subspace [4] and Generalized Principal Component Analysis (GPCA) [8], are designed for low-dimensional data, e.g., 3D point clouds. While handling the data with dimension in thousands or higher, these methods are nonetheless very expensive to compute. Also, these methods are lacking of robustness in dealing with noisy data. Several methods have been developed to improve their robustness and scalability, e.g., Median K-Flats [6] for K-Subspace and Robust Algebraic Segmentation (RAS) [33] for GPCA. Nevertheless, these improvements still possess no ability to deal with the gross errors (e.g., occlusions) widely existing in vision data.

It is now popular to perform subspace clustering by two computational steps: First, an $n \times n$ affinity matrix that encodes subspace membership is learnt from the given data matrix X . Then, the final clustering results are obtained by spectral clustering algorithms such as the Normalized Cut (NCut) [34], using the learnt affinity matrix as input. Many existing methods possess such a spectral nature, so called spectral-type methods. The main difference among various spectral-type methods is about learning the affinity matrix. In the ideal case where the subspaces are independent and the data is clean, Shape Interaction Matrix (SIM) [7] already provides a perfect estimate to the desired affinity matrix: Suppose the (skinny) SVD of X is $U\Sigma V^T$, then the row projector VV^T provably leads to correct clustering results [7, 13, 14]. However, in the presence of gross errors, the row projector VV^T computed with noisy data could be arbitrarily far from the authentic row projector, and thus $|VV^T|$ is no longer accurate as an affinity matrix for subspace clustering. To resolve this issue, Liu et al. [22] mathematically prove that, under certain conditions, the authentic row projector could be recovered by the following convex program, known as LRR:

$$\min_{Z, S} \|Z\|_* + \lambda \|S\|_{2,1}, \text{ s.t. } X = XZ + S, \quad (1)$$

where $\|\cdot\|_*$ and $\|\cdot\|_{2,1}$ are the nuclear norm (i.e., sum of singular values) and $\ell_{2,1}$ norm (sum of column-wise

ℓ_2 norms) of a matrix, respectively. Many extensions to LRR have been established and explored, e.g., Latent Low-Rank Representation (LatLRR) [16], Low-Rank Subspace Clustering (LRSS) [19] and Low-Rank Sparse Subspace Clustering (LRSSC) [14]. There also several methods that aim at obtaining some block-diagonal affinity matrices other than the row projector, e.g., Sparse Subspace Clustering (SSC) [10] and Spectral Curvature Clustering (SCC) [11].

Generally, spectral-type methods produce superior clustering results, but often run slowly, especially when the data dimension m and dataset size n are both large. More precisely, in the case of $m = n$, the construction of an $n \times n$ affinity matrix has $O(n^3)$ complexity, and the partition of an n -node graph into k clusters by NCut requires at least $O(n^2k + nk^2)$ time. Some methods have been proposed to improve the scalability of spectral-type methods, e.g., Scalable Sparse Subspace Clustering (SSSC) for SSC and the work of [21] for LRR. These two methods scale linearly to n , but suffer from the robustness issue and still have a quadratic dependence on m . Recently, a RANSAC-type method named Innovation Pursuit (IPursuit) [25] is proposed for fast subspace clustering. With the help of dimension reduction, IPursuit could scale linearly to both m and n , but still possesses no ability to identify the gross errors in data.

To reduce the running time, another key way is the so-called parallel algorithm, which divides a procedure into multiple pieces, executes those pieces on many devices in parallel and combines together multiple outputs at the end to get the correct result. Some substantial process has been made in this direction, e.g., [15]. The method proposed in this paper, as will be shown later, is easy to accelerate by parallel algorithm, because its most expensive step is about matrix multiplication.

3 PROBLEM FORMULATION AND ANALYSIS

Formally, the regime underlying a collection of points approximately drawn from a union of k subspaces could be described as $X = L_0 + S_0$, where L_0 stores the authentic samples lying exactly on the subspaces and S_0 corresponds to the possible errors. The word “error”, in general, refers to the deviation between the model assumption (i.e., subspaces) and the observed data. In practice, the errors could exhibit as white noise [35], missing entries [36], outliers [22, 37] and corruptions [30]. In this paper, we would like to focus on the setting of gross corruptions studied in PCP [30]; namely, S_0 is entry-wisely sparse and the values in S_0 are arbitrarily large.

As shown in [7, 13, 14], the row space (or row projector) of L_0 can lead to exact subspace clustering under certain conditions. Hence, Problem 1.1 would be mathematically formulated as a problem called *compressive row space recovery*:

Problem 3.1 (Compressive Row Space Recovery). *Let $L_0 \in \mathbb{R}^{m \times n}$ with SVD $U_0 \Sigma_0 V_0^T$ and rank r_0 store a set of n m -dimensional authentic samples strictly drawn from a union of k subspaces. Let $R \in \mathbb{R}^{p \times m}$ ($r_0 < p \ll m$) be a random Gaussian matrix. Suppose that the observed data matrix X is generated by $X = L_0 + S_0$, with S_0 being an entry-wisely sparse matrix corresponding to the possible errors. Denote $M \triangleq RX \in \mathbb{R}^{p \times n}$. Given M and R , the goal is to identify $V_0 V_0^T$ and S_0 .*

The above problem is essentially a generalization of the *subspace recovery* problem studied in [13]. To explore Problem 3.1, one may consider Compressive Sparse Matrix Recovery (CSMR) [38], which is a variation of Compressive Principal Component Pursuit (CPCP) [39]. Given M and R , CSMR strives to recover RL_0 and S_0 by convex optimization:

$$\min_{A \in \mathbb{R}^{p \times n}, S \in \mathbb{R}^{m \times n}} \|A\|_* + \lambda \|S\|_1, \text{ s.t. } M = A + RS, \quad (2)$$

where $\|\cdot\|_1$ denotes the ℓ_1 norm of a matrix seen as a long vector. Under certain conditions, it is provable that CSMR strictly succeeds in recovering both RL_0 and S_0 . However, as clarified in [38], CSMR is actually designed for the case where $m \gg n \gg r_0$, i.e., L_0 is a tall, low-rank matrix such that RL_0 is still low rank. In the cases of square or fat matrices, the recovery ability of CSMR is quite limited, because in this case RL_0 could be high rank or even full rank. To achieve better results, we shall devise a new method termed RSP, as will be shown in next section.

4 RSP AND SUBSPACE CLUSTERING

In this section, we shall detail the proposed RSP method for scalable and robust subspace clustering.

4.1 Compressive Row Space Recovery by RSP

The formula of RSP is derived as follows. Denote by $U_0 \Sigma_0 V_0^T$ and r_0 the SVD and rank of L_0 , respectively. Since $M = R(L_0 + S_0)$, we could construct a matrix $P \in \mathbb{R}^{n \times n}$ to annihilate L_0 on the right, i.e., $L_0 P = 0$. This can be easily done by taking $P = I - V_0 V_0^T$, with I being the identity matrix. That is,

$$(M - RS_0)(I - V_0 V_0^T) = RL_0(I - V_0 V_0^T) = 0. \quad (3)$$

Hence, we may seek both V_0 and S_0 by the following non-convex program termed RSP:

$$\begin{aligned} \min_{V \in \mathbb{R}^{n \times r}, S \in \mathbb{R}^{m \times n}} \|S\|_1, \\ \text{s.t. } (M - RS)(I - VV^T) = 0, V^T V = I, \end{aligned} \quad (4)$$

where $r_0 \leq r < p$ is taken as a hyper-parameter. To attain an exact recovery to the authentic row space V_0 , we would need $r = r_0$. Notice, that the equality in (3) always holds when V_0 is replaced by any other space that includes V_0 as a subspace. Thus, to obtain superior clustering results in practice, exact recovery

is not indispensable, and it is indeed unnecessary for the parameter r to strictly equal to the true rank r_0 , as will be shown in our experiments.

Analysis: We would like to provide an informal analysis for the RSP program (4). To this end, we first consider an equivalent version of (4):

$$\min_{P, S} \|S\|_1, \text{ s.t. } (M - RS)(I - P) = 0, P \in \Xi, \quad (5)$$

where $\Xi = \{VV^T : V \in \mathbb{R}^{n \times r}, V^T V = I\}$ is the set of orthogonal projections onto a r -dimensional row space. For simplicity, let $r = r_0$. Provided that $S = S_0$, $P = V_0 V_0^T$ will be the only feasible solution to the problem in (5). This is because, as long as $p \geq r_0$, it is almost surely that the row space of RL_0 (i.e., $M - RS_0$) is exactly V_0 . On the other hand, given $P = V_0 V_0^T$, the problem in (5) turns into a *sparse signal recovery* problem explored in [40]; that is,

$$\min_y \|y\|_1, \text{ s.t. } b = \Phi y, \quad (6)$$

where $\Phi = (I - V_0 V_0^T) \otimes R$ and $b = \text{vec}(M(I - V_0 V_0^T))$. Here, the symbols \otimes and $\text{vec}(\cdot)$ denote the Kronecker product and the vectorization of a matrix into a long vector, respectively. Since $I - V_0 V_0^T$ is an orthogonal projection, Φ may still satisfy the so-called Restricted Isometry Property (RIP) [40]. As a result, according to [40], the convex program in (6) may identify $\text{vec}(S_0)$ with overwhelming probability, as long as $p \geq c\|S_0\|_0/n$ holds for some numerical constant c , where $\|\cdot\|_0$ is the ℓ_0 pseudo-norm of a matrix, i.e., the number of nonzero entries of a matrix.

The above analyses illustrate that it is hopeful to mathematically prove that $(P = V_0 V_0^T, S = S_0)$ is a critical point to the non-convex problem in (5). However, due to the orthonormal constraint of $V^T V = I$, it would be hard to obtain a stronger guarantee. Thus, in this paper we would like to focus on the empirical performance of RSP. Still, the informal analysis presented above provides some useful clues for choosing the parameter p . Namely, to obtain exact or near exact recoveries to $V_0 V_0^T$ and S_0 , the parameter p has to satisfy the following two conditions:

$$p \geq r_0 \text{ and } p \geq c\|S_0\|_0/n. \quad (7)$$

For convenience, hereafter, we shall consistently refer to the quantity $\|S_0\|_0/n$ as the *corruption size*.

4.2 Optimization Algorithm

The observed data in reality is often contaminated by noise, and thus we shall consider instead the following non-convex program that can also approximately solve the problem in (4):

$$\min_{V \in \mathbb{R}^{n \times r}, S \in \mathbb{R}^{m \times n}} \lambda \|S\|_1 + \frac{1}{2} \|(M - RS)(I - VV^T)\|_F^2, \text{ s.t. } V^T V = I, \quad (8)$$

where $\|\cdot\|_F$ denotes the Frobenius norm of a matrix and $\lambda > 0$ is a hyper-parameter.

The optimization problem in (8) can be efficiently solved by any of the many first-order methods in the literature, e.g., Augmented Lagrange Multiplier (ALM) [41]. We would like to use the alternating proximal method studied in [42]. Let (V_t, S_t) be the solution estimated at the t th iteration. Denote

$$g(V, S) \triangleq \frac{1}{2} \|(M - RS)(I - VV^T)\|_F^2.$$

Then the solution to (8) is updated via iterating the following two procedures:

$$\begin{aligned} V_{t+1} &= \arg \min_V g(V, S_t), \text{ s.t. } V^T V = I, \\ S_{t+1} &= \arg \min_S \frac{\lambda}{\mu_t} \|S\|_1 + \frac{1}{2} \|S - (S_t - \frac{\partial_S g(V_{t+1}, S)}{\rho})\|_F^2, \end{aligned} \quad (9)$$

where $\rho > 0$ is a penalty parameter and $\partial_S g(V_{t+1}, S)$ is the partial derivative of $g(V, S)$ with respect to the variable S at $V = V_{t+1}$; namely,

$$\begin{aligned} \partial_S g(V_{t+1}, S) &= R^T (RS - M)(I - V_{t+1} V_{t+1}^T) \\ &= R^T (RS - RSV_{t+1} V_{t+1}^T - M + MV_{t+1} V_{t+1}^T). \end{aligned} \quad (10)$$

According to [42], the penalty parameter could be set as $\rho = 1.1\|R\|^2$, where $\|\cdot\|$ is the operator norm of a matrix, i.e., the largest singular value.

The two sub-problems in (9) both have closed-form solutions. More precisely, the V -subproblem is solved by finding the top r eigenvectors of a semi-positive definite matrix, $(M - RS_t)^T (M - RS_t)$. To do this, one actually just needs to calculate the top r right singular vectors of $M - RS_t$, which is a $p \times n$ matrix. The solution to the S -subproblem is given by

$$S_{t+1} = \mathcal{H}_{\lambda/\rho} [S_t - \frac{\partial_S g(V_{t+1}, S)}{\rho}], \quad (11)$$

where $\mathcal{H}_{\lambda/\mu_t}[\cdot]$ denotes the entry-wise shrinkage operator with parameter λ/ρ . The whole optimization procedure is also summarized in Algorithm 1. According to [42], Algorithm 1 can produce a converged solution within a finite number of iterations.

Algorithm 1 Solving the problem in (8) by the alternating proximal method

- 1: **input:** M, R, r and λ .
 - 2: **parameters:** $\rho = 1.1\|R\|^2$
 - 3: **Output:** V and S .
 - 4: **Initialization:** $S = 0$.
 - 5: **repeat**
 - 6: compute the matrix $M - RS$.
 - 7: update V using the top r right singular vectors of $M - RS$.
 - 8: compute the gradient given in (10).
 - 9: update S by (11).
 - 10: **until** convergence
-

4.3 Clustering Procedure

Given an estimate (denoted as \hat{V}_0) to the authentic row space V_0 , it is now rather standard to obtain the final subspace clustering results by using $|\hat{V}_0 \hat{V}_0^T|$ as an affinity matrix for spectral clustering. This approach often leads to superior clustering results, but is time consuming especially when n and k are both large. For the sake of high efficiency, we shall introduce a simple and efficient approach for obtaining the final clustering results based on the estimated row space, \hat{V}_0 , which is just an $n \times r$ ($r \ll n$) matrix.

Our approach is motivated by the following analyses. When the subspaces are independent and sufficient samples are observed for each subspace, it is known that $V_0 V_0^T$ is block-diagonal and can lead to correct clustering results [7, 13, 14]. In this case, actually, the $n \times r$ matrix V_0 also owns a structure of block-diagonal. To see why, assume without loss of generality that $L_0 = [L_1, L_2, \dots, L_k]$, where L_i with SVD $U_i \Sigma_i V_i^T$ is a matrix that stores the samples from the i th subspace. With these notations, it is easy to see that V_0 is equivalent to a block-diagonal matrix; namely, $V_0 = \tilde{V}_0 B$ with $B \in \mathbb{R}^{r \times r}$ being an orthogonal matrix (i.e., $BB^T = B^T B = I$) and

$$\tilde{V}_0 = \begin{bmatrix} V_1 & 0 & 0 & 0 \\ 0 & V_2 & 0 & 0 \\ 0 & 0 & \ddots & 0 \\ 0 & 0 & 0 & V_k \end{bmatrix}.$$

Given \tilde{V}_0 as above, correct clustering results could be obtained by using directly the K-Means algorithm to segment the rows of \tilde{V}_0 into k groups. Also, note that the orthogonal matrix B on the right strictly preserves the inner products among the row vectors. Thus, the clustering results are the same while using V_0 instead of \tilde{V}_0 as inputs to K-Means.

The above analyses illustrate that it is appropriate to get the final clustering results by applying directly K-Means onto the row vectors of \tilde{V}_0 . Algorithm 2 presents the whole procedure of the proposed subspace clustering method. Since the parameter λ depends on the operator norm of the sensing matrix R , we normalize R for the ease of choosing λ .

Algorithm 2 Subspace clustering by RSP

- 1: **input:** X and k .
 - 2: **parameters:** p , r and λ .
 - 3: **Output:** clustering results
 - 4: generate a $p \times m$ random Gaussian matrix R , and normalize R to be column-wisely unit-normed.
 - 5: compute $M = RX$.
 - 6: obtain \hat{V}_0 by Algorithm 1, using M, R, r and λ as the inputs.
 - 7: segment the row vectors of the $n \times r$ matrix \hat{V}_0 into k clusters by K-Means.
-

4.4 Computational Complexity

After obtaining \hat{V}_0 , the K-Means clustering step needs only $O(nkr)$ time and is often fast. So, most of the computational resources required by Algorithm 2 are consumed by its Step 6, i.e., Algorithm 1, which iteratively solves the RSP problem in (8).

Regarding Algorithm 1, its Step 6, i.e., the computation of the matrix $M - RS$, needs $pn + mnp$ elementary operations. The update of the variable V could be finished by computing the partial- r SVD of a $p \times n$ matrix and thus has a complexity of $O(pnr)$. To compute the gradient given in (10), $mnp + 4pnr + 4pn$ elementary operations are required. That is, Step 8, which is indeed the most expensive step in Algorithm 1, has an $O(mnp)$ complexity. The shrinkage operator used in Step 9 is computationally cheap, as it needs only $O(mn)$ time. In summary, each iteration in Algorithm 1 has an $O(mnp)$ complexity, and thereby the overall complexity of our Algorithm 2 is $O(mnpl + nkr)$, where l is the number of iterations required by Algorithm 1 to converge.

Up to present, the convergence rate of the alternating proximal method has not been fully understood. Empirically, we have found that at most 1000 iterations are needed for Algorithm 1 to produce near optimal solutions. So, it would be adequate to consider the computational complexity of our RPS as $O(mnp)$. Moreover, since the matrix multiplication operators are easily parallelizable, the proposed algorithms are indeed fairly fast, especially when running on Graphics Processing Unit (GPU).

Among the other things, it is worth noting that the iteration number l relates to the values of λ and r/p . In general, larger λ leads to more information loss and, accordingly, l will be smaller. For example, while λ is sufficiently large (e.g., $\lambda = +\infty$), the objective in (8) is perfectly minimized by $\hat{S}_0 = 0$, and in this case Algorithm 1 converges in only one iteration. Moreover, the iteration number l also depends on the value of r/p . In the extreme case of $r/p \geq 1$, Algorithm 1 runs only one iteration and outputs the solution of $\hat{S}_0 = 0$. Whenever $\hat{S}_0 = 0$, our RSP method is actually equivalent to applying SIM [7] onto the compressed matrix M .

5 EXPERIMENTS AND RESULTS

All experiments are conducted on a server equipped with a 64-bit Ubuntu 16.04 operating system, two Intel(R) Xeon(R) E5-2620 v4 2.10GHz CPU processors, 256GB RAM and four NVIDIA Titan X (Pascal) 12GB graphics cards. We have not implemented the algorithms using multiple GPU devices, and thus only one GPU card is randomly chosen by Matlab for accelerating the computations.

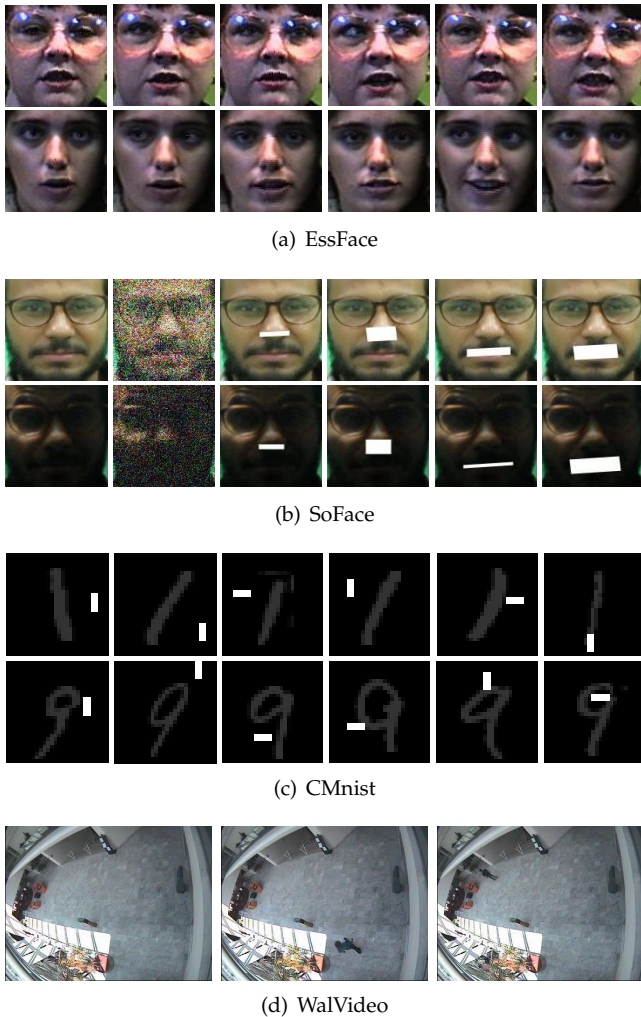


Fig. 1. Examples from the image datasets used in our experiments. The face or digit images in the same row across belong to the same class.

TABLE 1
Information about the five datasets used in the experiments of this paper .

name	#class (k)	#dimension (m)	#points (n)	#points in each class
SynMat	2	200	200	100
EssFace	375	10,000	7495	19~20
SoFace	2662	10,000	26,619	8~11
CMnist	10	784	70,000	6313~7877
WalVideo	n/a	27,648	1379	n/a

5.1 Experimental Settings

5.1.1 Experimental Data

To examine the effectiveness and efficiency of the proposed RSP method, we consider for experiments five datasets, including “SynMat”, “EssFace”, “SoFace”, “CMnist” and “WalVideo”:

1) SynMat: We first consider randomly generated matrices. A collection of 200×200 data matrices are generated according to the model of $X = L_0 + S_0$: L_0 is created by sampling 100 points from each of 2

randomly generated subspaces, and the values in each point are normalized such that the super norm of L_0 is 1; S_0 is consisting of random Bernoulli ± 1 values. The dimension of each subspace varies from 1 to 20 with step size 1, and thus the rank of L_0 varies from 2 to 40 with step size 2. The corruption size $\|S_0\|_0/n$ varies from 0.4 to 8 with step size 0.4. So, this dataset contains in total 400 matrices with size 200×200 .

2) EssFace: The images of the second dataset we used are provided by the University of Essex¹, so referred to as “EssFace”. This dataset contains in total 7495 images for 375 individuals, each of which has 19 or 20 images. The original images contain background, and no ground truth rectangle is provided. Thus, we utilize the face detector established in [43] to obtain the bounding boxes that contain only the faces. Then we resize the face rectangles into 100×100 , resulting in a collection of 7495 10,000-dimensional points for experiments. Figure 1(a) shows some examples from this dataset.

3) SoFace: The original SoF [44] dataset is a collection of 42,592 face images for 112 individuals, with each individual being involved in multiple photography sessions. The same physical setup is used in each session. The SoF dataset, in general, presents several challenges regarding face recognition, e.g., heavy noise, gross occlusion, strong expression, serious blurring and harsh illumination. Since the images for the same individual vary greatly in pose and appearance, it is hard, if not impossible, to form individual-level classes by using the pixel values as inputs for clustering. Thus, instead of identifying the individuals, we aim to group together the images from the same session, i.e., each session is treated as a class. Moreover, we resize the face rectangles into 100×100 and discard the images contaminated by blurring or canvas. For the ease of reference, we shall refer to this new version as “SoFace”, which defines a task of segmenting 26,619 data points with dimension 10,000 into 2662 classes. Some example images from this dataset are shown in Figure 1(b).

4) CMnist: We also consider the well-known MNIST [45] dataset, which is a collection of 70,000 images with size 28×28 for 10 handwritten digits. To test the robustness of subspace clustering methods, we corrupt each image by adding a “spot” with size 2×5 or 5×2 at a location chosen randomly from the image rectangle. The values in the spot are made to be 5 times as large as the maximum of pixel values so as to suppress the visual information of digits. For convenience, we refer to this corrupted version as “CMnist”, the images in which look like as shown in Figure 1(c).

5) WalVideo: In practice, the errors encoded in the sparse component S_0 could correspond to the objects of interest. To show this, we consider a surveillance

1. Available at cswwww.essex.ac.uk/mv/allfaces/index.html.

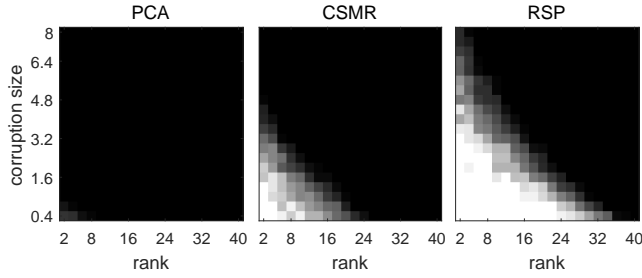


Fig. 2. Results in recovering the randomly generated matrices in SynMat. All the methods are performed on the compressed data matrix M with $p = 50$. The rank r_0 is assumed to be given. The numbers plotted in the above figures are averaged form 20 random trials.

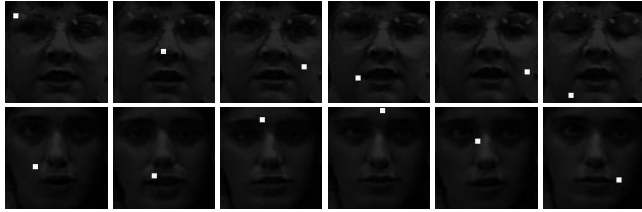


Fig. 3. Examples from the corrupted version of Ess-Face, with corruption size = 25.

video selected from the CAVIAR project². The video we considered is a sequence of 1379 frames taken in the entrance lobby of the INRIA Labs, recording the scenes in which one person is walking in straight line, so referred to as “WalVideo” (see Figure 1(d)). This video has a near static background, but contains dramatic illuminations. The original frames have a resolution 384×288 . We reduce the resolution by half so as to obtain a $27,648 \times 1379$ data matrix for experiments.

For the ease of reading, we summarize in Table 1 the major information of the above five datasets.

5.1.2 Baselines and Evaluation Metrics

For the sake of comparison, we implement 8 competing methods as follows.

- The proposed RSP method is closely related to SIM [7] and LRR [13]. Thus, we first consider to segment the original m -dimensional data points by SIM and LRR.
- Second, we apply the above two benchmark baselines, SIM and LRR, onto the compressed data matrix $M \in \mathbb{R}^{p \times n}$, resulting in another two competing methods termed “RP+SIM” and “RP+LRR”.
- Third, we carry out PCP [30] to try recovering L_0 from X at first, then apply subspace clustering methods onto the recovered matrix $\hat{L}_0 \in \mathbb{R}^{m \times n}$; this results in two baselines called “PCP+SIM” and “PCP+LRR”.

TABLE 2

Evaluation results on the corrupted version of EssFace, with corruption size 25. Except K-Means, for which GPU code runs slower than CPU code, all the other baseline codes are executed with GPU.

method	accuracy (%)	time (seconds)
K-Means*	7.65	1502
SIM	31.86	101
RP+SIM	12.25	67
PCP+SIM	64.23	84,821
CSMR+SIM	12.84	541
LRR	45.91	10,021
RP+LRR	7.45	142
PCP+LRR	65.19	91,586
CSMR+LRR	7.33	674
RSP (CPU)*	66.76(± 1.05)	1197(± 10)
RSP (GPU)	66.71(± 1.05)	280(± 2)

- Finally, we utilize CSMR [38] to try recovering $RL_0 \in \mathbb{R}^{p \times n}$ from M and apply subspace clustering methods onto the recovered $p \times n$ matrices; this also leads to two baselines, “CSMR+SIM” and “CSMR+LRR”.

Besides, we shall also report the results of K-Means clustering. Running time and clustering accuracy are used to evaluate the efficiency and effectiveness of subspace clustering methods, respectively. Here, the clustering accuracy is simply the percentage of correctly grouped data points.

5.1.3 Parameter Configurations

For the ease of choosing the parameters of various subspace clustering methods, first of all, we normalize the input matrix be column-wisely unit-normed. The parameter r in SIM plays the same role as in our RSP. So, first we manually tune r to maximize the accuracy of SIM, then we adjust r around this estimate for RSP. The parameter λ in RSP is chosen from the range of $2^{-10} \leq \lambda \leq 2^0$. For PCP, we follow the suggestion in [30] to set its regularization parameter as $\lambda = 1/\sqrt{\max(m, n)}$. Regarding CSMR, which is indeed sensitive to its regularization parameter λ , we try our best to test as more candidates as possible from the range $2^{-10}\|R\|/\sqrt{\max(p, n)} \leq \lambda \leq 2^{10}\|R\|/\sqrt{\max(p, n)}$, with the target of maximizing the accuracy of CSMR+SIM. Then the same parameter is used by the other CSMR based methods, e.g., CSMR+LRR. About the key parameter λ in LRR, we manually select a good estimate from the range of $0.1/\sqrt{\log n} \leq \lambda \leq 10/\sqrt{\log n}$.

5.2 Results on SynMat

As mentioned in Section 4.1, it is possible that RSP strictly succeeds in recovering $V_0V_0^T$ under certain conditions. To verify this, we first experiment with the SynMat dataset. For each pair of r_0 and $\|S_0\|_0/n$, we perform 20 random trials, and thus in this experiment we test 8000 matrices in total. To show the

2. Available at homepages.inf.ed.ac.uk/rbf/CAVIAR/.

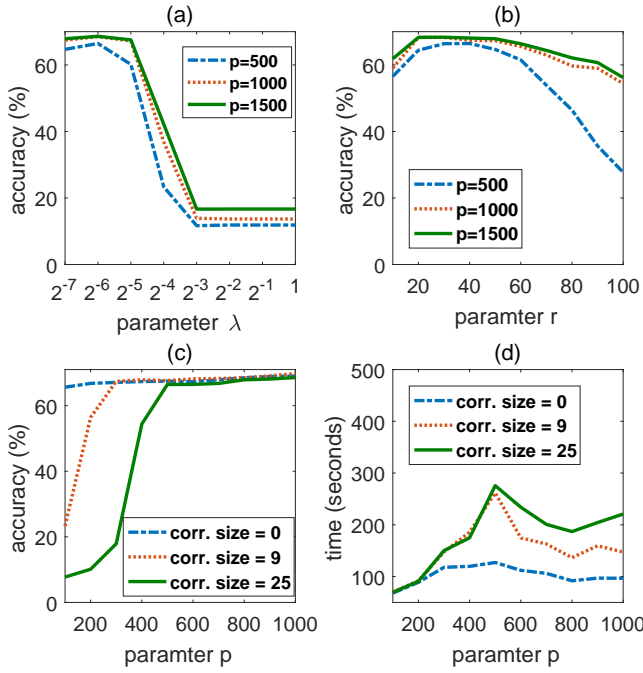


Fig. 4. Explore the performance of RSP under various parametric settings, using EssFace as the experimental data. (a) The parameter λ is varying while $r = 40$ and corruption size = 25. (b) The parameter r is varying while $\lambda = 2^{-6}$ and corruption size = 25. (c-d) The parameter p is varying while $\lambda = 2^{-6}$ and $r = 40$.

superiorities of RSP, we also consider to recover the target $V_0 V_0^T$ by PCA and CSMR: PCA estimates $V_0 V_0^T$ by computing directly the SVD of M , while CSMR is to firstly obtain an estimate to RL_0 by program (2) and then try to recover $V_0 V_0^T$ using the SVD of the estimate. The accuracy of recovery, i.e., the similarity between $V_0 V_0^T$ and $\hat{V}_0 \hat{V}_0^T$, is measured by Signal-to-Noise Ratio (SNR_{dB}).

The evaluation results are shown in Figure 2, in which each plotted number is a score defined as in the following:

$$\text{score} = \begin{cases} 0, & \text{SNR}_{\text{dB}} < 15, \\ 0.2, & 15 \leq \text{SNR}_{\text{dB}} < 20, \\ 0.5, & 20 \leq \text{SNR}_{\text{dB}} < 30, \\ 1, & \text{SNR}_{\text{dB}} \geq 30. \end{cases} \quad (12)$$

As we can see, PCA works poorly, attaining SNR_{dB} smaller than 15 in almost all the cases. This illustrates that it is unlikely to solve Problem 3.1 without accessing the sensing matrix R . Also, it can be seen that CSMR (with $p = 50$ and $\lambda = 1.2\|R\|/\sqrt{\max(p, n)}$) succeeds only in limited cases. The reason is that, as aforementioned, CSMR essentially requires $r_0 \ll \min(p, n)$ such that RL_0 is low rank. Our RSP does not suffer from this limit, and thereby RSP (with $p = 50$, $r = r_0$ and $\lambda = 2^{-7}$) can do much better than CSMR in recovering the authentic row space.

TABLE 3

Evaluation results on SoFace. Due to the memory limit of our GPU devices, some of the competing methods are only partially accelerated by GPU, and those methods are marked with asterisk.

method	accuracy (%)	time (seconds)
K-Means*	39.78	30,302
SIM	53.37	6118
RP+SIM	52.16	5806
PCP+SIM*	54.78	209,522
CSMR+SIM	53.82	6807
LRR*	60.16	77,961
RP+LRR	48.18	6996
PCP+LRR*	61.57	228,889
CSMR+LRR	48.01	8272
RSP (CPU)*	57.61(± 0.65)	1625(± 66)
RSP (GPU)	57.42(± 0.61)	528(± 8)

5.3 Results on EssFace

To get a comprehensive understanding about RSP, we corrupt each image by adding an $s \times s$ ($s = 0, 3, 5$) spot in a similar way as in CMnist (see Figure 3). Table 2 shows the comparison results at $s = 5$ (i.e., the corruption size is 25) and $p = 500$. Since this dataset contains only 7495 points, the SIM method, which only need to compute two SVDs, is fairly fast. However, SIM is not robust against gross corruptions and can therefore achieve only an accuracy about 32%. Even more, the situation becomes worse after pre-processing the data by random projection. LRR is better than SIM, but still produces an inferior accuracy about 45%. This is because LRR cannot handle the corruptions with very large magnitudes, as made clear in [22]. The pre-processing of PCP can dramatically improve the accuracy, but is quite time consuming; namely, PCP (using exact ALM) spends more than 23 hours in recovering L_0 . Benefiting from the compressive nature of the random projections, CSMR is computationally efficient. However, this method fails to make any improvement in terms of clustering accuracy. The reason is probably that $p = 500$ is too small, and in this case CSMR cannot get a good estimate to RL_0 . Our RSP (with $p = 500$, $r = 40$ and $\lambda = 2^{-6}$) attains an accuracy about 67% within 5 minutes (the iteration number is 1000). This confirms the high efficiency and robustness of RSP.

We also investigate the influences of the parameters in RSP. As shown in Figure 4(a), the accuracy of RSP drops dramatically when $\lambda \geq 2^{-4}$. This is because, as aforementioned, RSP will produce the trivial solution of $\hat{S}_0 = 0$ if λ is sufficiently large. Provided that there is no dense noise in the data, theoretically speaking, there exists $\lambda^* > 0$ such that RSP works equally well for all $\lambda \leq \lambda^*$. However, in practice the white noise always exists, and thus the performance of RSP is slightly suppressed while λ is too small. Overall, $\lambda = 2^{-6}$ is a good choice for this dataset. Regarding the parameter r , Figure 4(b) shows that RSP could work equally well while r locates in a certain range.

TABLE 4

Evaluation results on CMnist. The methods that use no GPU device are marked with asterisk.

method	accuracy (%)	time (seconds)
K-Means*	18.12	1634
SIM*	12.36	3680
RP+SIM*	11.24	3674
PCP+SIM*	53.67	11,705
CSMR+SIM*	11.24	7620
LRR*	10.97	6020
RP+LRR *	10.55	4165
PCP+LRR*	54.61	12,700
CSMR+LRR*	10.56	7990
RSP (CPU)*	50.74 (± 2.53)	2023(± 104)
RSP (GPU)	50.65 (± 2.61)	620(± 108)

This confirms our doctrine that r is unnecessary to strictly equal to r_0 . For this dataset, $r = 40$ is a proper setting, as can be seen from Figure 4(b). Figure 4(c) shows that RSP breaks down while p is too small, and the value of the breaking point depends on the corruption size. More precisely, without the gross corruptions, RSP actually works equally well for a wide range of p . In the case where the corruption size is 9, RSP breaks down when $p \leq 200$. When the corruption size increases to 25, the breaking point becomes $p \leq 400$. These phenomena, in general, are consistent with the statement in (7). Figure 4(d) plots the running time as a function of the parameter p . Note that the running time is unnecessary to increase monotonically as the enlargement of p . Because, as aforementioned, the number of the iterations required by Algorithm 1 to converge actually depends on p .

5.4 Results on SoFace

In terms of running time, as shown in Table 3, RSP (with $p = 500$, $r = 120$ and $\lambda = 2^{-5}$) distinctly outperforms all the competing methods. In particular, RSP is even much faster than RP+SIM, which is to simply apply SIM onto the compressed matrix $M \in \mathbb{R}^{500 \times 26,619}$. This is because SoFace has a large number of data points and classes, saying $n = 26,619$ and $k = 2662$. In this case, spectral clustering is indeed very slow due to the following two procedures: 1) computing the partial SVD of an $n \times n$ matrix, and 2) using K-Means to segment a collection of n k -dimensional points into k clusters. Our Algorithm 1 converges with about 400 iterations, and after that, in sharp contrast, Algorithm 2 only needs to perform K-Means clustering on a set of n r -dimensional points. Besides of its high efficiency in computation, RSP is also memory saving and can be therefore fully accelerated by our GPU device, which has a memory limit of 12GB.

In a sense of clustering accuracy, LRR based methods may outperform our RSP. The reason is that LRR can somehow capture the *extra structures beyond subspaces* [46], which are also useful for clustering.

TABLE 5

Running time on WalVideo. The parameters of RSP are set as $r = 5$ and $\lambda = 2^{-6}$

method	time (seconds)	
	CPU	GPU
PCP	4606	2820
RSP ($p = 1000$)	1024	301
RSP ($p = 2000$)	1755	469
RSP ($p = 3000$)	2299	511

5.5 Results on CMnist

Different from EssFace and SoFace, CMnist has a structure of considerably nonlinear; namely, the digits are not aligned well, as can be seen from Figure 1(c). Yet, it is still acceptable to apply subspace clustering methods onto this dataset, as a low-dimensional manifold can often be covered by a subspace with dimension slightly higher than that of the manifold [2]. Anyway, here our main aim is to test the efficiency of RSP in the case where X is a fat matrix.

The evaluation results are shown in Table 4. Since the data dimension is only 784, dimension reduction may not improve dramatically the computational efficiency. Interestingly, as we can see, our RSP (with $p = 300$, $r = 20$ and $\lambda = 2^{-6}$) is still faster than the competing methods. In particular, when using GPU, RSP is even several times faster than K-Means. This is not weird, because the last step of our Algorithm 2 only needs to perform K-Means clustering on a set of r -dimensional points, the computational load of which is much lower than using K-Means to segment the original 784-dimensional data.

5.6 Results on WalVideo

Unlike the above clustering experiments, in this experiment the input matrix M is not normalized, and thus it is suitable to visualize the sparse component \hat{S}_0 produced by RSP. Figure 5 shows four frames taken from the WalVideo dataset, which has dramatic illuminations in background. As we can see, RSP with $p \geq 2000$ works almost as well as PCP. Moreover, in terms of stability against the illumination in background, RSP is even slightly better than PCP. To be more precise, PCP occasionally treats a considerable amount of background illumination as the moving objects (see the second row of Figure 5), while RSP produces more reliable results for the same frame. Since in this dataset the data matrix X is tall (i.e., $m \gg n$), the computational complexity of RSP and PCP has the same order. Yet, as shown in Table 5, RSP is still faster than PCP, especially when GPU is used. Our RSP is more parallelizable than PCP, and thus RSP benefits more from GPU than PCP does.

Besides of its superiorities in computational efficiency, RSP might be useful in reducing the storage and communication cost in Internet video analysis. More precisely, the sender compresses their videos by

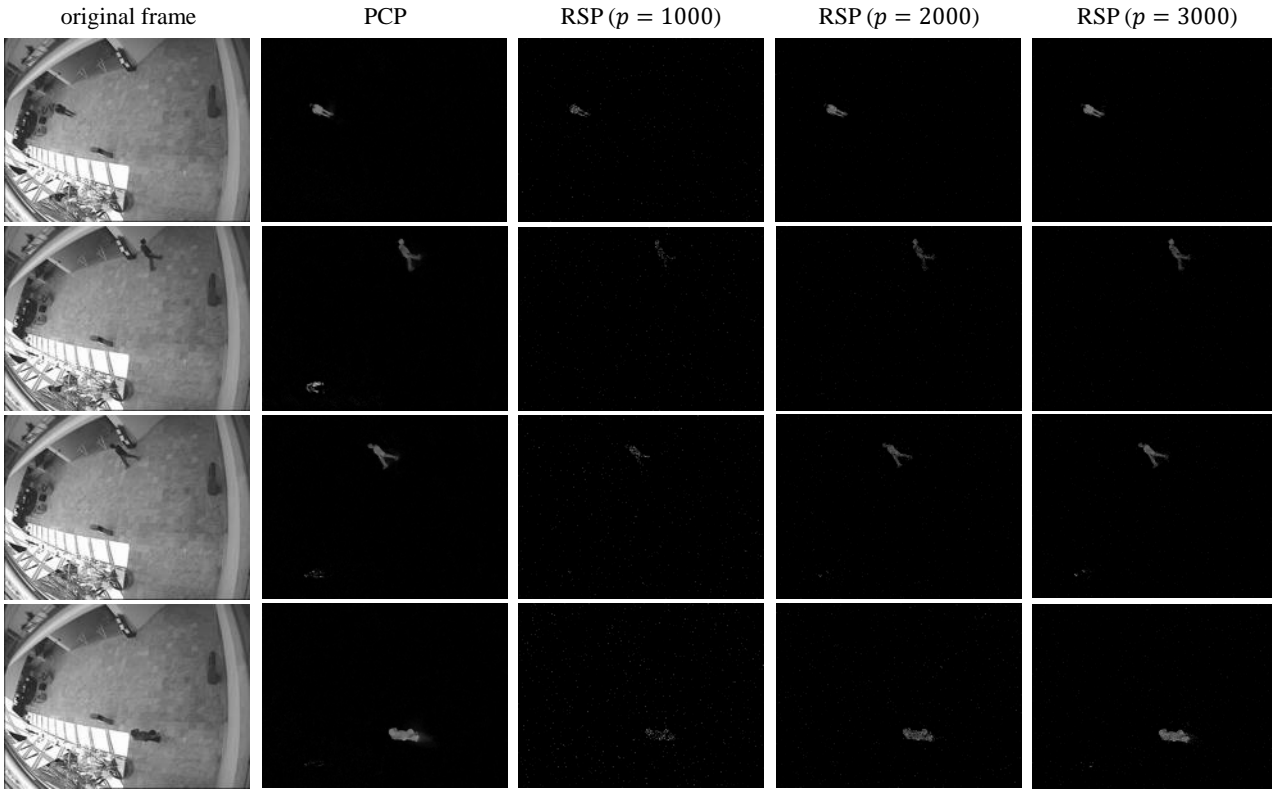


Fig. 5. Moving object detection in surveillance video. Four frames from the WalVideo dataset, with varying illumination. From left to right: the original frame, the sparse component $|\hat{S}_0|$ obtained by PCP and RSP. The parameters in RSP are set as $r = 5$ and $\lambda = 2^{-6}$.

random projection before transferring data through Internet, and the receiver could analyze the compressed data by RSP.

6 CONCLUSION

For the purpose of scalable and robust subspace clustering, in this paper we studied the problem of *compressive robust subspace clustering*, a significant problem not thoughtfully explored before. We first mathematically formulated the problem as to recover the row space of the clean data, given only the compressed data M and sensing matrix R . Then we devised a novel method termed RSP, which iteratively seeks both the authentic row space and the sparse errors existing in the original high-dimensional data. Extensive experiments with various settings verified the scalability and robustness of RSP.

ACKNOWLEDGEMENT

This work is supported in part by national Natural Science Foundation of China (NSFC) under Grant 61622305, Grant 61502238, Grant 61532009, Grant 61672292, Grant 61432019 and Grant 71490725, in part by Natural Science Foundation of Jiangsu Province of China (NSFJPC) under Grant BK20160040, in part by the Six Talent Peaks Project of Jiangsu Province under

Grant DZXX-037, in part by the Key University Science Research 320 Project of Jiangsu Province under Grant 15KJA520001.

REFERENCES

- [1] R. Vidal, "Subspace clustering," *IEEE Signal Processing Magazine*, vol. 28, no. 3, pp. 52–68, 2011.
- [2] M. Soltanolkotabi and E. Candes, "A geometric analysis of subspace clustering with outliers," *Ann. Statist.*, vol. 40, no. 4, pp. 2195–2238, 2012.
- [3] M. Fischler and R. Bolles, "Random sample consensus: A paradigm for model fitting with applications to image analysis and automated cartography," *Communications of the ACM*, vol. 24, no. 6, pp. 381–395, 1981.
- [4] J. Ho, M. Yang, J. Lim, K. Lee, and D. Kriegman, "Clustering appearances of objects under varying illumination conditions," in *IEEE Conference on Computer Vision and Pattern Recognition*, vol. 1, 2003, pp. 11–18.
- [5] A. Gruber and Y. Weiss, "Multibody factorization with uncertainty and missing data using the EM algorithm," in *IEEE Conference on Computer Vision and Pattern Recognition*, vol. 1, 2004, pp. 707–714.
- [6] T. Zhang, A. Szlam, and G. Lerman, "Median k-flats for hybrid linear modeling with many outliers," in *International Conference on Computer Vision Workshops*, 2009, pp. 234 – 241.

- [7] J. Costeira and T. Kanade, "A multibody factorization method for independently moving objects," *International Journal of Computer Vision*, vol. 29, no. 3, pp. 159–179, 1998.
- [8] Y. Ma, A. Yang, H. Derksen, and R. Fossum, "Estimation of subspace arrangements with applications in modeling and segmenting mixed data," *SIAM Review*, vol. 50, no. 3, pp. 413–458, 2008.
- [9] Y. Ma, H. Derksen, W. Hong, and J. Wright, "Segmentation of multivariate mixed data via lossy data coding and compression," *IEEE Transactions on Pattern Analysis and Machine Intelligence*, vol. 29, no. 9, pp. 1546–1562, 2007.
- [10] E. Elhamifar and R. Vidal, "Sparse subspace clustering," in *IEEE Conference on Computer Vision and Pattern Recognition*, vol. 2, 2009, pp. 2790–2797.
- [11] G. Chen and G. Lerman, "Spectral curvature clustering (scc)," *Int. J. Comput. Vision*, vol. 81, pp. 317–330, 2009.
- [12] G. Liu, Z. Lin, and Y. Yu, "Robust subspace segmentation by low-rank representation," in *International Conference on Machine Learning*, 2010, pp. 663–670.
- [13] G. Liu, Z. Lin, S. Yan, J. Sun, Y. Yu, and Y. Ma, "Robust recovery of subspace structures by low-rank representation," *IEEE Transactions on Pattern Analysis and Machine Intelligence*, vol. 35, no. 1, pp. 171–184, 2013.
- [14] Y.-X. Wang, H. Xu, and C. Leng, "Provable subspace clustering: When lrr meets ssc," in *Advances in Neural Information Processing Systems 26*, C. J. C. Burges, L. Bottou, M. Welling, Z. Ghahramani, and K. Q. Weinberger, Eds., 2013, pp. 64–72.
- [15] A. Talwalkar, L. Mackey, Y. Mu, S. F. Chang, and M. I. Jordan, "Distributed low-rank subspace segmentation," in *IEEE International Conference on Computer Vision*, 2013, pp. 3543–3550.
- [16] G. Liu and S. Yan, "Latent low-rank representation for subspace segmentation and feature extraction," in *ICCV*, 2011.
- [17] C.-Y. Lu, H. Min, Z.-Q. Zhao, L. Zhu, D.-S. Huang, and S. Yan, "Robust and efficient subspace segmentation via least squares regression," in *European Conference on Computer Vision*. Berlin, Heidelberg: Springer-Verlag, 2012, pp. 347–360.
- [18] M. Soltanolkotabi, E. Elhamifar, and E. Candes, "Robust subspace clustering," *Ann. Statist.*, vol. 42, no. 2, pp. 669–699, 2014.
- [19] P. Favaro, R. Vidal, and A. Ravichandran, "A closed form solution to robust subspace estimation and clustering," in *IEEE Conference on Computer Vision and Pattern Recognition*, 2011, pp. 1801–1807.
- [20] X. Peng, L. Zhang, and Z. Yi, "Scalable sparse subspace clustering," in *IEEE Conference on Computer Vision and Pattern Recognition*, 2013, pp. 430–437.
- [21] X. Zhang, F. Sun, G. Liu, and Y. Ma, "Fast low-rank subspace segmentation," *IEEE Transactions on Knowledge and Data Engineering*, vol. 26, no. 5, pp. 1293–1297, 2014.
- [22] G. Liu, H. Xu, J. Tang, Q. Liu, and S. Yan, "A deterministic analysis for LRR," *IEEE Transactions on Pattern Recognition and Machine Intelligence*, vol. 38, no. 3, pp. 417–430, 2016.
- [23] G. Liu, Q. Liu, and P. Li, "Blessing of dimensionality: Recovering mixture data via dictionary pursuit," *IEEE Transactions on Pattern Recognition and Machine Intelligence*, vol. 39, no. 1, pp. 47–60, 2017.
- [24] X. Peng, S. Xiao, J. Feng, W.-Y. Yau, and Z. Yi, "Deep subspace clustering with sparsity prior," in *International Joint Conference on Artificial Intelligence*. AAAI Press, 2016, pp. 1925–1931.
- [25] M. Rahmani and G. Atia, "Innovation pursuit: A new approach to the subspace clustering problem," in *International Conference on Machine Learning*, vol. 70, 2017, pp. 2874–2882.
- [26] C. Lu, J. Feng, Z. Lin, T. Mei, and S. Yan, "Subspace clustering by block diagonal representation," *IEEE Transactions on Pattern Analysis and Machine Intelligence*, vol. PP, no. 99, pp. 1–1, 2018.
- [27] G. Liu and S. Yan, "Active subspace: Toward scalable low-rank learning," *Neural Computation*, vol. 24, no. 12, pp. 3371–3394, 2012.
- [28] S. A. Shah and V. Koltun, "Robust continuous clustering," *Proceedings of the National Academy of Sciences*, vol. 114, no. 37, pp. 9814–9819, 2017.
- [29] E. J. Candes and M. B. Wakin, "An introduction to compressive sampling," *IEEE Signal Processing Magazine*, vol. 25, no. 2, pp. 21–30, 2008.
- [30] E. J. Candès, X. Li, Y. Ma, and J. Wright, "Robust principal component analysis?" *Journal of the ACM*, vol. 58, no. 3, pp. 1–37, 2011.
- [31] X. Mao and Y. Gu, "Compressed subspace clustering: A case study," in *IEEE Global Conference on Signal and Information Processing*, 2014, pp. 453–457.
- [32] A. Ruta and F. Porikli, "Compressive clustering of high-dimensional data," in *2012 11th International Conference on Machine Learning and Applications*, vol. 1, 2012, pp. 380–385.
- [33] S. Rao, A. Yang, S. Sastry, and Y. Ma, "Robust algebraic segmentation of mixed rigid-body and planar motions in two views," *International Journal of Computer Vision*, vol. 88, no. 3, pp. 425–446, 2010.
- [34] J. Shi and J. Malik, "Normalized cuts and image segmentation," *IEEE Transactions on Pattern Analysis and Machine Intelligence*, pp. 888–905, 2000.
- [35] E. Candès and Y. Plan, "Matrix completion with noise," *IEEE Proceeding*, vol. 98, pp. 925–936, 2010.
- [36] G. Liu, Q. Liu, and X. Yuan, "A new theory for

- matrix completion," in *Advances in Neural Information Processing Systems*. Curran Associates, Inc., 2017, pp. 785–794.
- [37] G. Liu, H. Xu, and S. Yan, "Exact subspace segmentation and outlier detection by low-rank representation," *Journal of Machine Learning Research - Proceedings Track*, vol. 22, pp. 703–711, 2012.
 - [38] M. Mardani, G. Mateos, and G. B. Giannakis, "Recovery of low-rank plus compressed sparse matrices with application to unveiling traffic anomalies," *IEEE Trans. Inf. Theor.*, vol. 59, no. 8, pp. 5186–5205, 2013.
 - [39] J. Wright, A. Ganesh, K. Min, and Y. Ma, "Compressive principal component pursuit," in *IEEE International Symposium on Information Theory*, 2012, pp. 1276–1280.
 - [40] E. J. Candes and T. Tao, "Decoding by linear programming," *IEEE Transactions on Information Theory*, vol. 51, no. 12, pp. 4203–4215, 2005.
 - [41] Z. Lin, M. Chen, L. Wu, and Y. Ma, "The augmented Lagrange multiplier method for exact recovery of corrupted low-rank matrices," UIUC Technical Report UILU-ENG-09-2215, Tech. Rep., 2009.
 - [42] H. Attouch and J. Bolte, "On the convergence of the proximal algorithm for nonsmooth functions involving analytic features," *Mathematical Programming*, vol. 116, no. 1-2, pp. 5–16, 2009.
 - [43] K. Zhang, Z. Zhang, Z. Li, and Y. Qiao, "Joint face detection and alignment using multitask cascaded convolutional networks," *IEEE Signal Processing Letters*, vol. 23, no. 10, pp. 1499–1503, 2016.
 - [44] M. Afifi and A. Abdelhamed, "Afif4: Deep gender classification based on adaboost-based fusion of isolated facial features and foggy faces," *Arxiv*, vol. PP, 2017.
 - [45] Y. Lecun, L. Bottou, Y. Bengio, and P. Haffner, "Gradient-based learning applied to document recognition," *Proceedings of the IEEE*, vol. 86, no. 11, pp. 2278–2324, 1998.
 - [46] G. Liu and P. Li, "Low-rank matrix completion in the presence of high coherence," *IEEE Transactions on Signal Processing*, vol. 64, no. 21, pp. 5623–5633, 2016.